Evidence for strong flux pinning by small, dense nanoprecipitates in a Sm-doped $YBa_2Cu_3O_{7-\delta}$ coated conductor

Xueyan Song,[a] Zhijun Chen, Sang-Il Kim, D. Matthew Feldmann, and David Larbalestier
Applied Superconductivity Center, University of Wisconsin-Madison, Madison, Wisconsin 53706

Jodi Reeves, Yiyuan Xie, and Venkat Selvamanickam
SuperPower Incorporated, Schenectady, New York 12304

(Received 22 November 2005; accepted 28 April 2006; published online 25 May 2006)

About 17 vol. % of ~10 nm sized $(Y,Sm)_2O_3$ precipitates have been developed in a metal-organic chemical vapor deposition grown Sm-doped $YBa_2Cu_3O_{7-\delta}$ coated conductor. The precipitate spacing of ~15 nm suggests strong vortex-precipitate pinning interactions, which are evidenced by a shift in the peak in the flux pinning force curve, an enhanced irreversibility field exceeding 8 T at 77 K, and a lack of temperature scaling of the flux pinning force over the temperature range of 65–82 K. © *2006 American Institute of Physics*. [DOI: 10.1063/1.2206989]

Remarkably it has been recently shown that high densities of second phase particles which enhance the flux pinning can be introduced into $YBa_2Cu_3O_{7-\delta}$ (YBCO) using pulsed laser deposition (PLD) with alternating multilayers[1,2] or whole-target composition modification.[3–5] However, more practical routes to coated conductors (CC) employ techniques such as metal-organic deposition (MOD),[6] physical vapor deposition (PVD),[7] and metal-organic chemical vapor deposition (MOCVD),[8] for which the incorporation of fine secondary phase nanoparticles needs better understanding. Rare-earth doping of the YBCO is being evaluated as one promising method, both to form second phase particles,[8] as well as to induce point defects by cation exchange between the rare-earth element and Ba.[9] A striking enhancement of J_c, in a coated conductor rather than a research sample, both at self and at high fields, was found by Selvamanickam *et al.*[8] using a 10% substitution of the large rare-earth ion Sm (radius=0.119 nm vs 0.109 nm) for Y. For example, they reported $J_c(0\ T, 75.5\ K)$ values of 1.0 and 2.3 MA/cm^2 for pure and Sm-doped CCs, while Kramer function extrapolations of the $J_c(H)$ data suggested irreversibility fields of 7.1 and 11.8 T, respectively. In this letter, we focus on the detailed microstructural and electromagnetic properties of this MOCVD-grown 10%Sm substituted YBCO CC which explains its enhanced flux pinning. As is common to most such CC production processes,[10] the YBCO shows some thickness variability and macroscopic defects that can block current, making J_c less well defined by the quotient I_c/A, where A is the average YBCO cross section, than for most research samples. We first show the dense and fine nanostructures from which strong flux pinning is to be expected and then discuss the electromagnetic signatures of this strong vortex pinning.

This MOCVD CC (Ref. 8) had a nominal composition of $Y_{0.9}Sm_{0.1}Ba_2Cu_3O_x$ and was grown on an ion-beam-assisted deposition (IBAD) template of Y_2O_3-stabilized ZrO_2 (YSZ). Focused ion beam (FIB) cross sections and transmission electron microscopy (TEM) plan-view sections showed that the average YBCO thickness of 1.03 μm varied by 10%–15% over a length of the order of 10 μm and, most importantly for the precipitated phases found within the YBCO, that the YBCO layer also incorporated ~20 vol % of Ba–Cu–O amorphous, nonsuperconducting regions which sometimes clumped in regions that were up to half the film thickness, thus significantly impeding current flow. The

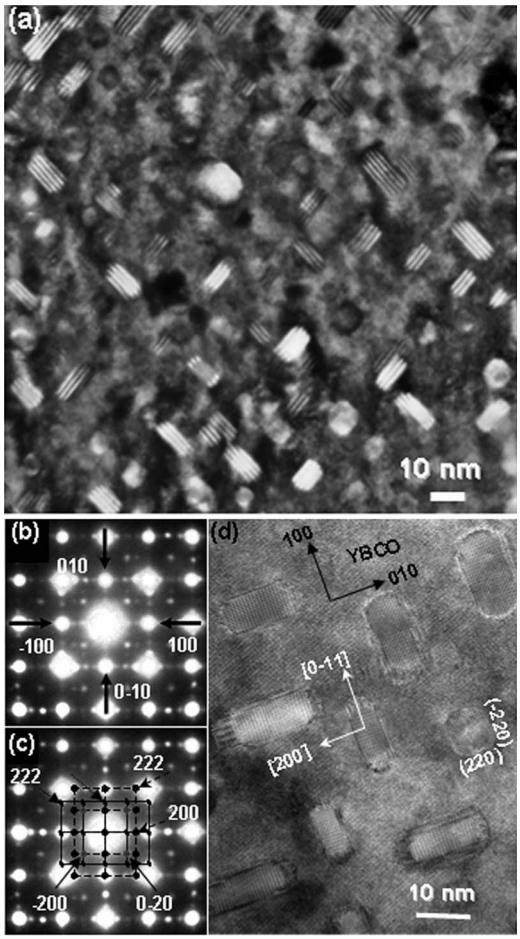

FIG. 1. (a) TEM plan-view diffraction contrast showing the nanoprecipitate array within YBCO grain. (b) Complex electron diffraction taken along the [001] axis of YBCO grain. (c) Index of complex electron diffraction shown in Fig. 1(b). The solid arrows indicate the diffraction spots from the square shaped precipitates. The dashed and dotted arrows indicate the diffraction spots from two sets of rectangular shaped precipitates. (d) High resolution TEM image showing the faceting of the nanoprecipitates.

[a]Electronic mail: xsong@wisc.edu

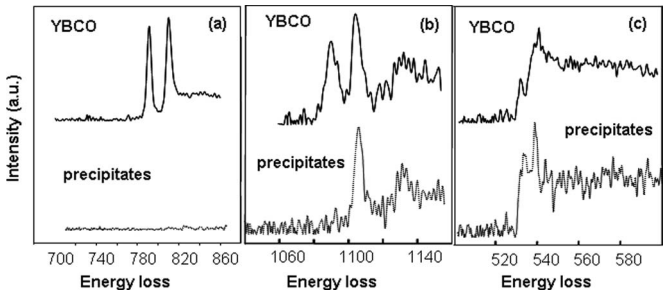

FIG. 2. (a) EELS of Ba $M_{5,4}$ edge from both the nanoprecipitates and YBCO. (b) EELS of Sm $M_{5,4}$ edge from both the nanoprecipitates and YBCO. (c) EELS of Oxygen K edge from both the nanoprecipitates and YBCO.

YBCO texture was excellent, the in-plane full width at half maximum ($\Delta\phi$) being 3.7° and the out-of plane ($\Delta\omega$) 1.0°, suggesting little or no limitation of J_c by grain boundary effects.[11,12] Plan-view TEM samples were prepared by mechanical polishing and ion milling. Diffraction contrast and high resolution TEM imaging were performed in a Philips CM200, while the nanoscale chemistry was analyzed using a 0.2 nm probe and on-axis electron energy loss spectroscopy (EELS) with an energy dispersion of 0.2 eV per channel and an energy resolution of ~0.8 eV in a JEOL 2010F scanning transmission electron microscope (STEM). Transport properties were measured on laser-cut bridges ~60 μm wide by ~500 μm long to restrict I_c to <3 A so as to permit 1 μV/cm J_c measurements down to 65 K in magnetic fields up to 9 T. The superconducting transition temperature and normal state resistivity were measured during slow cooling. The irreversibility field $H^*(T)$ was defined by the linear extrapolation of the Kramer pinning function $J_c^{-1/2}B^{1/4}$ to zero.

Plan-view diffraction contrast images [Fig. 1(a)] taken at different YBCO depths show a dense (~17 vol %) and uniform distributed nanoprecipitate array within all YBCO grains. The precipitates are ~10 nm in size and spaced by 10–15 nm with area and volume densities of $\sim 3.5 \times 10^{11}$ cm^{-2} and $\sim(5-6)\times 10^{16}$ cm^{-3}. The primary diffractions of YBCO are complicated by diffractions from the nanoprecipitates [Fig. 1(b)]. The precipitates are body-centered cubic with a lattice parameter of $a_0 \sim 10.7$ Å. They grow with well-defined orientation relationships to the YBCO, [Fig. 1(c)], square shaped precipitates exhibit relationship $[001]_{ppt}//[001]_{YBCO}$, $(-200)_{ppt}//(110)_{YBCO}$, and rectangular shaped precipitates are either $[0-11]_{ppt}//[001]_{YBCO}$, $(110)_{ppt}//(010)_{YBCO}$, and $(200)_{ppt}//(100)_{YBCO}$, or $[0-11]_{ppt}//[001]_{YBCO}$, $(100)_{ppt}//(-100)_{YBCO}$, and $(200)_{ppt}//(010)_{YBCO}$. Contrast changes near the precipitate edges in the higher magnification image in Fig. 1(d) are due to the wedge-shaped interface between the precipitates and the YBCO. The rectangular precipitates all lie with their long axis parallel to either $(100)_{YBCO}$, or $(010)_{YBCO}$ and grow along the orientation of the smallest lattice mismatch with the YBCO. For example, the mismatch between $(200)_{ppt}$ (~3.7 Å) and $(100)_{YBCO}$ (~3.81 Å) is less than 2%.

Local energy dispersive x-ray (EDX) compositional analysis in the STEM showed Y in the precipitates, while the EELS Ba $M_{5,4}$ edges from YBCO grains and precipitates in Fig. 2(a) clearly indicate that the precipitates do not contain Ba. EELS of the Sm $M_{5,4}$ and the O K edges in Figs. 2(b) and 2(c) show Sm and O in both YBCO and precipitates. Sm, Y, and O are found together in the precipitates and do not form any compound with the structure different from that of Sm_2O_3 and Y_2O_3, which are both bcc with lattice parameters of Sm_2O_3=10.927 Å, Y_2O_3=10.604 Å. Figure 2(c) shows that the shape of the oxygen K edge in the precipitates is the same as that found for Y_2O_3 grains,[13] while the hole preedge seen in the YBCO (Ref. 14) is of course very different. Hence we index the precipitates as $(Y,Sm)_2O_3$. Y_2O_3 precipitates of similar size and density were earlier found in Y-enriched nonstoichiometric YBCO films and associated with enhanced vortex pinning too.[15,16] Consistent with the minority substitution of Y by Sm, a_0 (precipitates=10.7 Å) is much closer to that for Y_2O_3.

Evaluation of the superconducting properties has both engineering and scientific aspects. From an engineering point of view, this conductor is distinguished by a rather high critical current (187 A/cm width) at a thickness of 1.03 μm and a T_c of 90 K, making this a very competitive coated conductor.[8] Here we want to focus on the vortex pinning significance of the very fine precipitate structure shown in Fig. 1. However, using the average YBCO thickness to define J_c does not immediately suggest strong vortex pinning because this defines the self-field 77 K J_c as 1.7 MA/cm^2, a respectable but far from the record coated conductor J_c value. Several issues need to be addressed in assessing raw values of the self-field J_c. One is that the evaluation should be made between samples of similar thickness grown with the same YBCO deposition technique. As noted above, the self-field J_c value of the Sm-doped YBCO CC is indeed about 2.3 times the pure YBCO CC.[8] A second issue, rather harder to assess, is the impact of the thickness variation and the Ba–Cu–O amorphous phase on the cross section actively carrying current, which affects the magnitude of the local current density that is representative of the flux pinning current density. In a parallel study of rather porous MOD CC,[10] we used the normal state resistivity ρ to renormalize the cross section. The high value of ρ (300 K) of 354 $\mu\Omega$ cm and the linear resistivity curve from RT to T_c are consistent with optimally doped YBCO, for which ρ (300 K) should be ~250 $\mu\Omega$ cm.[17] The simplest conclusion is that only ~70% of the average thickness of 1.03 μm is actually available for current flow due to the obstruction by Ba–Cu–O amorphous phase, which is too large for effective flux pinning, but is necessary to balance the overall film composition, accounting for the ~17 vol % $(Y,Sm)_2O_3$ observed in Fig. 1. Since the MOCVD process is inherently flexible with respect to reactant supply,[8] it is likely that this amorphous phase can be eliminated, resulting in a higher J_c due to a greater effective superconducting cross section.

Figure 3(a) plots the average thickness $J_c(H)=I_c/A$ curves. $J_c(H)$ stays high in the midfield range and the irreversibility field attains 8.4 T at 77 K, considerably higher than for most research samples and for CC films made by MOD.[18] In fact, there was significant excess J_c above 8.4 T and a smooth extrapolation of the Kramer function to zero suggested H^* (77 K) ~9.5 T, a value agreeing within 0.2 T with the field at which J_c=100 A/cm^2. To check for the influence of the dense pinning array on the flux pinning properties, we checked the temperature scaling of the pinning force $F_p(H)$ and find that it does not exhibit temperature scaling, as is common with coated conductors.[19] Figure 3(b)

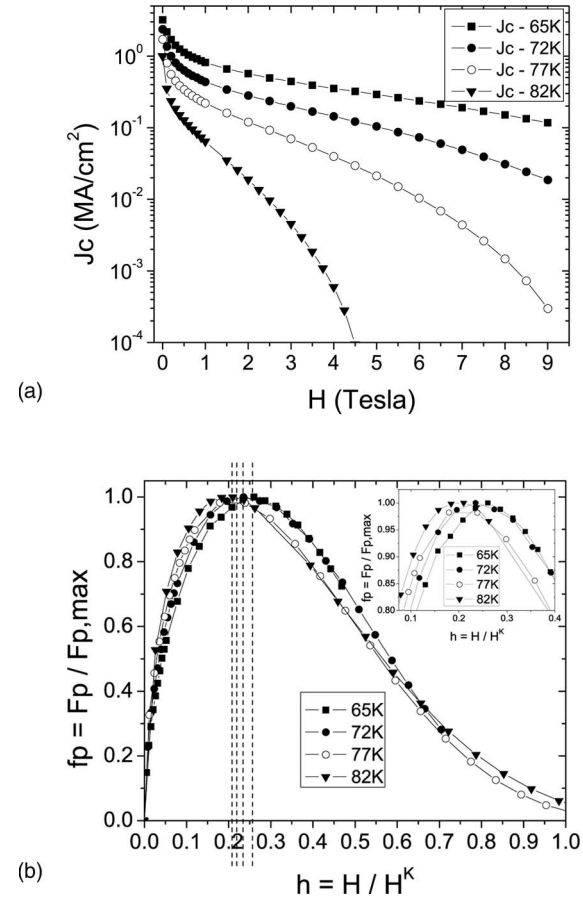

FIG. 3. (a) Critical current density J_c defined as I_c/A at 65–82 K. (b) Reduced bulk pinning force curves at 65–82 K.

shows a progressive shift of the pinning force peak position from reduced fields $h=H/H^*=0.21$ (0.8 T) at 82 K to $h=0.26$ at 65 K (5 T) as the temperature is lowered. Since the vortex spacing $a=(\phi_0/B)^{0.5}$ equals the mean precipitate spacing of ~15 nm only at a field of 10 T, just above our maximum measuring field, we expect that the vortex pinning efficiency should continuously improve for all temperatures down to that at which the irreversibility field is ~10 T. Consistent with this picture and in marked disagreement with recent studies of the low field α pinning parameter $J_c \propto H^{-\alpha}$ in various CC (Refs. 20 and 21) where a temperature-independent parameter of around 0.5 is reported, here we find that α continuously decreases from −0.625 at 82 K to −0.395 at 50 K. These signatures are all consistent with the conclusion that, at least up to fields of ~10 T at which the areal vortex density starts to exceed the areal precipitate density, progressively stronger pinning efficiency with decreasing temperature occurs.

These data reinforce a point made by other recent work showing that Sm is a very benefical constituent of $REBa_2Cu_3O_{7-x}$.[4,5] Matsumoto *et al.*[4] found that very high flux pinning can be developed in pure Sm-123, perhaps due to the nanoscale phase separation produced by the Sm–Ba site interchange, a possible explanation also advanced by MacManus-Driscoll *et al.*[5] in their study of a 50%Sm substituted YBCO film. They also advanced the possibility of linear defects such as dislocations emanating from such nanoscale defects, as seen much more explicitly in their study of the positive influence of $BaZrO_3$ precipitates on the flux pinning. We did indeed search for the evidence of dislocations in our images but did not find them. It seems likely that the smaller 10%Sm doping of this sample expresses itself most directly through the production of the significant Ba- and Cu-rich phases and its balancing RE_2O_3 precipitate array, whose density and spacing is responsible for the lack of nonscaling of the flux pinning force seen in Fig. 3(b).

In summary we have reported here both microstructural and electromagnetic evidences for an enhanced vortex pinning in Sm substituted MOCVD coated conductors which produces ~17 vol % of mixed $(Y,Sm)_2O_3$ particles that are ~10 nm in size and separated by ~15 nm. Such precipitate arrays can be a powerful way to enhance the critical current density and high-field performance of coated conductors.

This work was supported by the Air-Force Office of Scientific Research through the MURI.

[1] T. Haugan, P. N. Barnes, R. Wheeler, F. Meisenkothen, and M. Sumption, Nature (London) **430**, 867 (2004).
[2] J. Hänisch, C. Cai, R. Hühne, L. Schultz, and B. Holzapfel, Appl. Phys. Lett. **86**, 122508 (2005).
[3] J. L. Macmanus-Driscoll, S. R. Foltyn, Q. X. Jia, H. Wang, A. Serquis, L. Civale, B. Maiorov, M. E. Hawley, M. P. Maley, and D. E. Peterson, Nat. Mater. **3**, 440 (2004).
[4] K. Matsumoto, T. Horide, A. Ichinose, S. Horii, Y. Yoshida, and M. Mukaida, Jpn. J. Appl. Phys., Part 2 **44**, 246 (2005).
[5] J. L. MacManus-Driscoll, S. R. Foltyn, B. Maiorov, Q. X. Jia, H. Wang, A. Serquis, L. Civale, Y. Lin, M. E. Hawley, M. P. Maley, and D. E. Peterson, Appl. Phys. Lett. **86**, 032505 (2005).
[6] M. W. Rupich, D. T. Verebelyi, W. Zhang, T. Kodenkandath, and X. Li, MRS Bull. **29**, 572 (2004).
[7] R. Feenstra, A. A. Gapud, F. A. List, E. D. Specht, D. K. Christen, T. G. Holesinger, and D. M. Feldmann, IEEE Trans. Appl. Supercond. **15**, 2803 (2005).
[8] V. Selvamanickam, Y. Xie, J. Reeves, and Y. Chen, MRS Bull. **29**, 579 (2004).
[9] J. L. MacManus-Driscoll, S. R. Foltyn, Q. X. Jia, H. Wang, A. Serquis, B. Maiorov, L. Civale, Y. Lin, M. E. Hawley, M. P. Maley, and D. E. Peterson, Appl. Phys. Lett. **84**, 5329 (2004).
[10] S. Kim, A. Gurevich, D. M. Feldmann, X. Song, X. Li, W. Zhang, T. Kodenkandath, M. W. Rupich, T. G. Holesinger, and D. C. Larbalestier, Supercond. Sci. Technol. (unpublished).
[11] D. T. Verebelyi, D. K. Christen, R. Feenstra, C. Cantoni, A. Goyal, D. F. Lee, M. Paranthaman, P. N. Arendt, R. F. DePaula, J. R. Groves, and C. Prouteau, Appl. Phys. Lett. **76**, 1755 (2000).
[12] D. M. Feldmann, J. L. Reeves, A. A. Polyanskii, G. Kozlowski, R. R. Biggers, R. M. Nekkanti, I. Maartense, M. Tomsic, P. Barnes, C. E. Oberly, T. L. Peterson, S. E. Babcock, and D. C. Larbalestier, Appl. Phys. Lett. **77**, 2906 (2000).
[13] A. Travlos, N. Boukos, G. Apostolopoulos, and A. Dimoulas, Appl. Phys. Lett. **82**, 4053 (2003).
[14] Xueyan Song, George Daniels, Matt Feldmann, Alex Gurevich, and David Larbalestier, Nat. Mater. **4**, 470. (2005).
[15] P. Lu, Y. Q. Li, J. Zhao, C. S. Chern, B. Gallois, P. Norris, B. Kear, and F. Cosandey, Appl. Phys. Lett. **60**, 1265 (1992).
[16] A. Catana, R. F. Broom, J. G. Bednorz, J. Mannhart, and D. G. Schlom, Appl. Phys. Lett. **60**, 1016 (1992).
[17] D. K. Fork, F. A. Ponce, J. C. Tramontana, N. Newman, Julia M. Phillips, and T. H. Geballe, Appl. Phys. Lett. **58**, 2432 (1991).
[18] S. Kim, D. M. Feldmann, D. T. Verebelyi, C. Thieme, X. Li, A. A. Polyanskii, and D. C. Larbalestier, Phys. Rev. B **71**, 104501 (2005).
[19] T. Kiss, M. Inoue, S. Nishimura, T. Kuga, T. Matsushita, Y. Iijima, K. Kakimoto, T. Saitoh, S. Awaji, and K. Watanabe, Physica C **382**,: 57 (2002).
[20] L. Civale, B. Maiorov, A. Serquis, J. O. Willis, J. Y. Coulter, H. Wang, Q. X. Jia, P. N. Arendt, M. Jaime, J. L. MacManus-Driscoll, M. P. Maley, and S. R. Foltyn, J. Low Temp. Phys. **135**, 87 (2004).
[21] L. Civale, B. Maiorov, A. Serquis, J. O. Willis, J. Y. Coulter, H. Wang, Q. X. Jia, P. N. Arendt, J. L. MacManus-Driscoll, M. P. Maley, and S. R. Foltyn, Appl. Phys. Lett. **84**, 2121 (2004).